Folding Paper Shopping Bags*

Devin J. Balkcom† Erik D. Demaine‡ Martin L. Demaine‡ John A. Ochsendorf§
Zhong You¶

Abstract

One of the most ubiquitous examples of origami is the common paper shopping bag. In a common model of paper folding, there are a finite number of creases, between which the paper must stay rigid and flat, as if made of plastic or metal plates connected by hinges. We show that (maybe surprisingly), the paper shopping bag cannot be flattened under this model using the usual pattern of creases. This raises the question of what foldings are possible in this model? We introduce some techniques for foldability analysis, and show that the bag may be flattened by adding new creases, or by adding new material between creases.

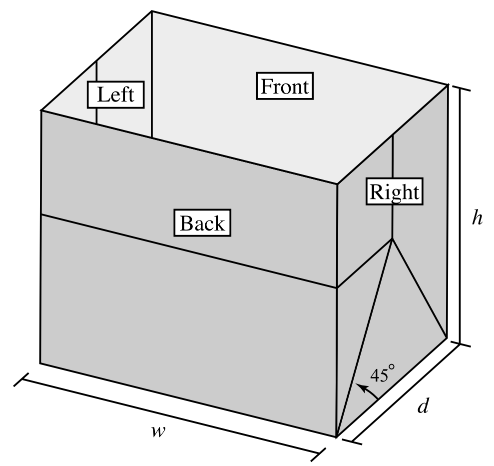

Figure 1: A shopping bag with the traditional crease pattern.

1 Introduction

In grocery stores around the world, people fold and unfold countless paper bags every day. The rectangular-bottomed paper bags that we know today are manufactured in their 3D shape, then folded flat for shipping and storage, and later unfolded for use. This process was revolutionized by Margaret Knight (1838–1914), who designed a machine in 1867 for automatically gluing and folding rectangular-bottomed paper bags [11]. Before then, paper bags were cut, glued, and folded by hand. Knight's machine effectively demolished the working-class profession of "paper folder".

Our work questions whether paper bags can be truly (mathematically) folded and unfolded in the way that happens many times daily in reality. More precisely, we consider foldings that use a finite number of creases, between which the paper must stay rigid and flat, as if the paper were made of plastic or metal plates connected by hinges. Such foldings are sometimes called *rigid origami*, being more restrictive than general origami foldings, which allow continuous bending and curving of the paper and thus effectively uncountably infinite "creasing". It is known that essentially everything can be folded by a continuous origami folding [6], but that this is not the case for rigid origami.

We prove that the rectangular-bottomed paper bag cannot be folded flat or unfolded from its flat state using the usual set of creases that are so common in reality—in fact, the bag cannot move at all from either its folded or unfolded state.

The difficulty with folding can be removed by shortening the bag – for example, by making a horizontal cut all the way around the bag at a height of $d/2$, with dimensions as shown in figure 1. The pattern of creases on the shortened bag resembles that of cardboard boxes department stores use to pack sweaters or collared shirts.

One way to understand the difference between short bags and tall bags is to make a vertical cut along the edge between the right and back sides of the bag, and another along the edge between the left and back sides. As the cut bag is folded, the cut sides separate from each other by as much as $22°$. Adding additional paper between the cut

*A preliminary version of parts of this paper was presented at the 14th Annual Fall Workshop on Computational Geometry, November 2004.

†Dartmouth Computer Science Department, Pittsburgh, PA 15213, devin@cs.dartmouth.edu

‡MIT Computer Science and Artificial Intelligence Laboratory, 32 Vassar St., Cambridge, MA 02139, USA, {edemaine,mdemaine}@mit.edu

§School of Architecture, MIT, 77 Massachusetts Ave., Cambridge, MA 02139 USA

¶Department of Engineering Science, Parks Road, Oxford, zhong.you@eng.ox.ac.uk

edges might therefore allow the bag to be folded.

Finally, we prove that rigid folding is possible without adding paper. If all of the dimensions of the bag are equal, then the pattern of diagonal creases shown in figure 10(b) can be used to 'twist' the bag flat. If the dimensions are not equal, a sequence of 'telescoping' folds as shown in figure 12 shorten the bag until it can be collapsed.

2 Related Work

In the mathematical literature, the closest work to rigid folding is *rigidity*. The famous Bellows Theorem of Connelly, Sabitov, and Walz [4] says that any polyhedral piece of paper forming a closed surface preserves its volume when folded according to a finite number of creases. In contrast, as suggested by the existence of bellows in the real world, it is possible to change the volume using origami folding. Even more fundamental are Cauchy's rigidity theorem, Aleksandrov's extension, and Connelly's extension [2], which all establish an inability to fold a convex polyhedron using a finite number of creases. (In Cauchy's case, the creases must be precisely the edges of the polyhedron; in Connelly's case, any finite set of additional creases can be placed; Aleksandrov's theorem is somewhere in between.) Another result of Connelly[1] is that a positive-curvature "corner" (the cycle of facets surrounding a vertex in a convex polyhedron) cannot be turned "inside-out" no matter how we place finitely many additional creases; this result answers a problem of Gardner [7]. In contrast, a paper bag can be turned inside-out with an origami folding (and in real life) [3].

Few papers discuss rigid origami directly. Demaine and Demaine [5] present a family of origami "bases" that can be folded rigidly. Streinu and Whiteley [15] proved that any single-vertex crease pattern can be folded rigidly—up to but not included the moment at which multiple layers of paper coincide. Balkcom and Mason [1] demonstrate how some classes of origami can be rigidly folded by a robot.

Huffman [9] and McCarthy [12] derive equations describing the relationship between angles of four creases that meet at a vertex. Hull and Belcastro [14] describe the relationship for vertices where several creases intersect using a product of rotation matrices; we solve these equations explicitly to compute three dependent crease angles as a function of the other crease angles.

If a rigid folding is possible, the equations relating crease angles must have a solution along the entire folding trajectory. The connectedness of the space of solutions has been analyzed by Kapovich and Millson [10]; our approach is based on work on planar closed chains by Milgram and Trinkle [13].

[1] Personal communication, 1998.

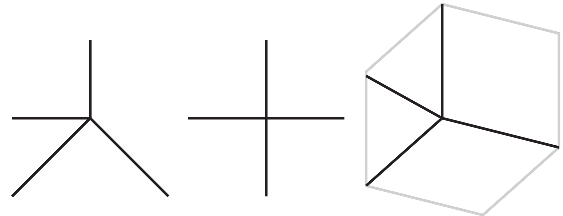

Figure 2: The three types of vertex found in a shopping bag.

3 Model and Definitions

We take a simple polyhedral model of the shopping bag. The facets are rigid and infinitely thin; facets may become coplanar during folding, but are not permitted to pass through one another. Creases are assumed to be line segments, and their positions relative to the facets that they bound are fixed.

Several creases may meet at a vertex; we will call the angles between adjacent creases meeting at a vertex *sector angles*, and call the angles between adjacent facets across a crease *dihedral angles*. The sector angles depend on the design of the bag, which we will call the *crease pattern*, while the dihedral angles describe the current configuration of the bag.

4 Non-foldability of the Traditional Crease Pattern

Figure 1 shows the traditional crease pattern for a shopping bag. The height of the bag is h, the width is w, and the depth is d. We assume that $h > d/2$; this ensures that the diagonal creases on the right and left sides of the bag meet.

We can distinguish three types of vertex; see figure 2. The vertices in the middle of each of the right and left sides of the bag have sector angles of $(90°, 135°, 90°, 45°)$. There is a vertex along each of the two of the upright edges of the bag, with sector angles $(90°, 90°, 90°, 90°)$. There are vertices at the corners of the bag with sector angles $(90°, 90°, 45°, 45°)$.

Some pairs of vertices share a crease; figure 3 shows how vertices of each type are connected to one another.

The sequence of sector angles around a vertex determine a relationship between the dihedral angles at creases around the vertex. Huffman [9] derives a relationship between opposite dihedral angles m and n for a degree-four

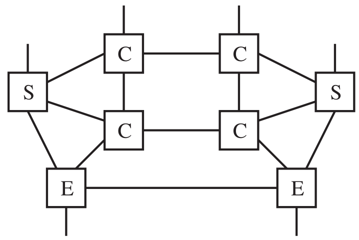

Figure 3: The vertex graph for a shopping bag. The nodes represent 'edge', 'side', and 'corner' vertices, and the edges represent creases that connect vertices.

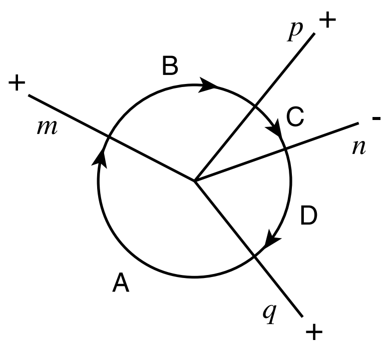

Figure 4: Huffman's notation for the relationship between four creases. A, B, C, and D are sector angles; m, n, p, and q are the dihedral angles.

vertex,

$$1 - \cos n = \frac{\sin A \sin B}{\sin C \sin D}(1 - \cos m), \tag{1}$$

where A, B, C, and D are sector angles as shown in figure 4.

For both *side* and *edge* vertices, $A + C = 180°$, and $B + D = 180°$. Equation 1 can be simplified:

$$\cos n = \cos m. \tag{2}$$

We can use this relationship between dihedral angles to show that a shopping bag with the traditional crease pattern cannot be rigidly folded.

Theorem 1 *A shopping bag with the traditional crease pattern cannot be rigidly folded.*

Proof: Consider an 'edge' vertex. The two vertical creases that meet at this vertex have crease angles that are equal in magnitude; if the magnitude is not 0 or π, then the two horizontal creases from this vertex must be one of $\{0, \pi\}$. Choose a crease that is 0 or π, and connected to another vertex. Walk the crease network; each of the left and right sides is flat (open or folded), and each of the corners is either fully open or collapsed. ■

5 Folding Short Bags

On each of the left and right sides of the traditional shopping bag, there are two creases that make a $45°$ angle with the bottom edge. If $h \leq d/2$, then the creases on each side do not intersect on the interior of the facet; we say the bag is *short*.

Short bags, unlike tall bags with the traditional crease pattern, can be rigidly folded flat. The proof has three components. First, we conjecture a solution: a continuous trajectory of dihedral angles that starts with the open configuration and ends at a flat configuration. We then show that the solution is topologically consistent – *i.e.*, that at all configurations along the trajectory satisfy the constraints among crease angles imposed by the geometry of the paper and the crease pattern. Finally, we show that the paper does not pass through itself at any point along the trajectory.

5.1 Configuration-space Topology

The configuration of a rigid origami mechanism is completely determined by the dihedral angles, but not all choices of dihedral angles satisfy the constraints imposed by the geometry of the paper and the crease pattern.

Finding a trajectory from start to goal that satisfies the constraints can be difficult. The space of configurations may have multiple components, or sections of the configuration space may be joined only at specific regions along their boundaries. For the tall shopping bag described, the possible configurations are 'fully open' and 'fully closed'; the configuration space is a pair of isolated points.

In this section, we describe a geometric method for analyzing the connectedness of the configuration space for a single vertex at the intersection of four creases; this method is based on work by Trinkle and Milgram [16]. If the configuration space has only one component, then there exists a topologically consistent path between every pair of start and goal configurations.

The technique can also be used to determine whether a given path is topologically consistent. For the purposes of this analysis, we allow paper to pass through itself; we deal with self-intersections separately in the foldability proofs below.

Figure 5 shows an example. We first cut the paper along one of the creases, as shown. If the crease angles were known for creases 1 and 2, then the configuration of the mechanism would be completely determined. However, there is an additional constraint – that the crease angles of the uncut creases be such that the edges of the cut crease 'line up'. We will therefore analyze the behavior of a point on the cut crease (points A and B in the figure), and see how it restricts motion of the other creases.

We label the creases as shown in figure 5, cut crease 3, and rigidly attach the facet between creases 1 and 4 to the ground. Consider the motion of the point A as the paper is allowed to fold along creases 1 and 2. Point A is a fixed distance from the central vertex, and can move on the surface of a sphere. Its motion is also bounded on the left by a plane normal to crease 1, and containing point A. There are two configurations of crease angles 1 and 2 that allow point A to reach most locations on the sphere: crease 2 may be convex, or concave. There are some locations that can only be reached in one way: those that fall on the plane normal to crease 1 and containing point A. There is also one point that can be reached in an infinite number of ways, at the intersection of crease 1 and the sphere.

Now consider point B, that rotates around crease 4. The reachable locations form a circle that lies in a plane perpendicular to crease 4.

If the cut is removed, point A and point B must touch; we will call this point AB. AB must move on the intersection of the sphere cut by a plane that A moves on, and the circle that B moves on. The locations that AB can reach therefore form an arc of a circle.

We can describe the space of possible configurations of the paper by the ways in which point AB can reach each point on the arc. There are two configurations that reach each point on the interior of the arc (crease 2 may be either concave or convex). There is only one way in which each of the endpoints of the arc can be reached – crease 2 is flat at each endpoint.

Each point on the arc corresponds to a slice of the space of configurations of the paper, described by crease angles 1 and 2. Starting at one endpoint of the arc, the slice is a single configuration. Moving continuously along the arc, each new slice corresponds to two configurations. At the final slice (at the other endpoint of the arc), there is only one configuration. The topology of this shape, and thus of the configuration space, is a circle – a 1-dimensional manifold with one component.

In general, the set of reachable locations of point A is a sphere bounded by two planes perpendicular to crease 1. The intersection of this surface with the circle reachable by point B can be a circle, an arc of a circle, or two arcs of a circle. Depending on the shape of this workspace, and the ways in which point AB can reach each point on the workspace, the configuration space may have one of several different structures, as shown in figure 6.

- *Null intersection*. One side of the circle may be completely contained in the workspace. The pre-image of an arc completely contained within the workspace is two arcs.

- *Transverse intersection*. One side of the circle may

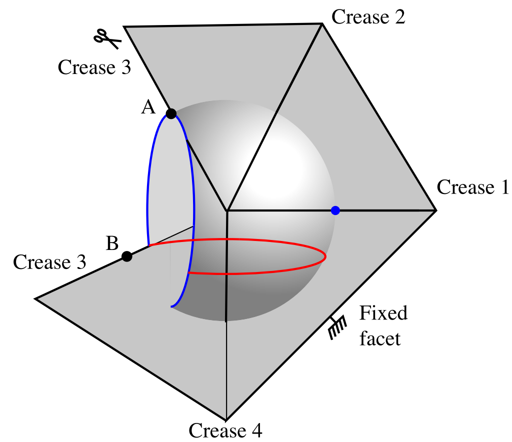

Figure 5: A degree-four vertex, cut along crease 3.

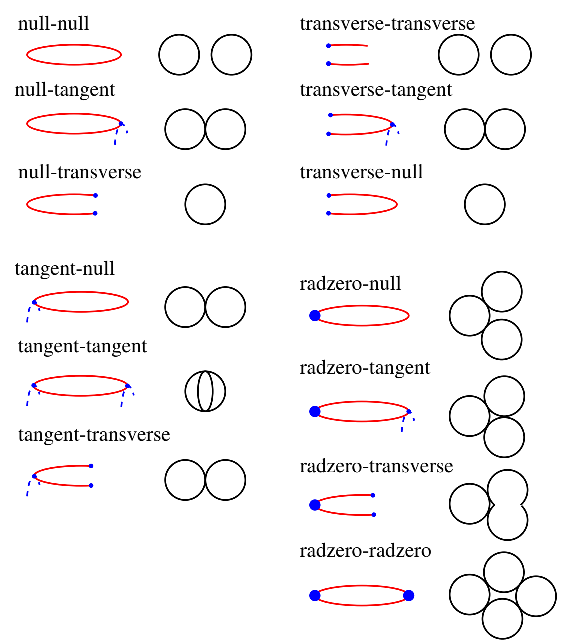

Figure 6: Thirteen of the sixteen possible ways a circle can intersect the workspace of an open three-bar spherical chain. For each class, the ellipses on the left show the workspace; the circles on the right show the configuration space (the pre-image of the workspace). There are seven distinct topological classes of configuration space.

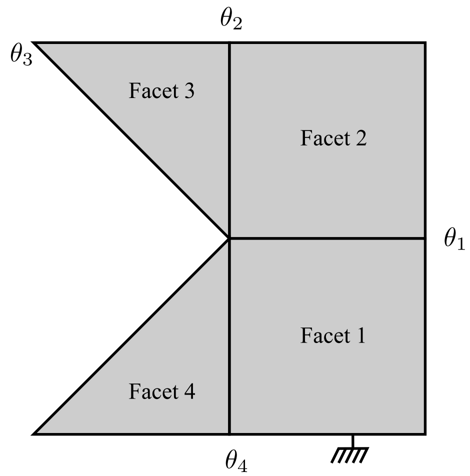

Figure 7: A corner of the short bag, cut between two facets, and anchored to the ground.

be cut by the bounding plane at two points. The pre-image of an arc touching the bounding plane is an arc.

- *Tangent intersection*. The circle just touches a bounding circle of non-zero radius. The pre-image of an arc tangent to the bounding circle is a pair of arcs touching at a single interior point.
- *Radius-zero intersection*. The circle touches the bounding plane at one of the poles of the sphere on the x axis. The pre-image of this point is a circle of configurations corresponding to spinning links about the x axis; the pre-image of an arc through this point is two arcs connected by a circle.
- We ignore the case where the circle is completely contained within the boundary of the open workspace.

5.2 Proof of Foldability

Theorem 2 *Every short shopping bag can be rigidly collapsed.*

Proof: Consider a corner vertex. If we ignore self-intersections, we can see that the configuration space is a single connected component as follows. Let the links be numbered as shown in figure 7, and anchor link 1. The workspace of the endpoint of link 3 is the portion of the sphere bounded by two halfplanes; $|x| < \sqrt(2)/2$. The workspace of the endpoint of link 4 is a circle of radius $\sqrt(2)/2$, centered at the point $(0, -1)$. The pre-image of the intersection of these two workspaces is a pair of circles connected at two points. (These points correspond to two collapsed configurations.)

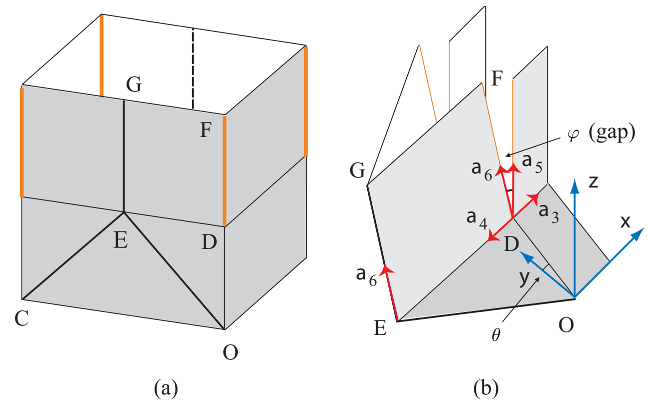

Figure 8: A tall bag. (a) the crease pattern and (b) partially folded bag when some of the edges are cut open.

We choose the collapsed configuration in which all dihedral angles are π, and choose a trajectory that moves to this configuration directly (*i.e.*, without passing through the other collapsed trajectory). We let θ_1 increase monotonically from $\pi/2$ to π. From equation 1, $\theta_2 = \pm\theta_4$; for the trajectory we have chosen, $\theta_2 = \theta_4$. θ_1 also increases monotonically from $\pi/2$ to π for this trajectory.

Adjacent facets can only collide if the angle between them is zero or π; no crease angles are 0 or π except at the start and end of the trajectory. Intersections between facets 1 and 3 must first occur when the θ_2 or θ_3 axis touches the $z = 0$ plane; since θ_1 and θ_4 are positive except at the end of the trajectory, there are no intersections. The case of intersection between facets 2 and 4 is symmetric.

The four corners of the bag are connected by creases along the bottom of the bag, and all four corners fold occur simultaneously and symmetrically; the condition that $h \leq d/2$ is sufficient to ensure that no facets that do not share a vertex can intersect. ∎

6 Folding Tall Bags

Short bags can be folded; this suggests several techniques for folding taller bags. We consider adding new paper between creases, and adding more creases.

6.1 Folding by Adding Material

Figure 8a shows a bag whose height is greater than $d/2$. Three horizontal creases have been added at a height of $d/2$, forming a complete rectangle of creases that circumscribe the bag. Experimenting with a card model reveals that the edges of the bag turn to split open during the folding. In other words, gaps, as those shown in figure 8b, appear during the folding process. We can compute the size of the gaps.

Consider a tall bag with edges above height $d/2$ being cut open. Figure 8 shows a partially folded bag. A set of vectors, a_3, a_4, a_5, and a_6, are introduced to present the creases and the edges of panels that are slit open. We choose a right-handed Cartesian coordinate system as shwn, with origin at vertex O, the x axis along the bottom front edge, and the y axis in the plane of the bottom of the bag.

$$a_3 = (1, 0, 0) \tag{3}$$

$$a_4 = \frac{OE - OD}{|OE - OD|} = (-\cos\delta, 1 - \cos\theta, \sin\delta - \sin\theta). \tag{4}$$

Since the slit edges are perpendicular to both FD and DH, $a_3 \cdot a_5 = 0$, and $a_4 \cdot a_6 = 0$. Therefore,

$$a_5 = (0, \cos\omega, \sin\omega) \tag{5}$$

$$a_6 = \left(\frac{\sin\delta - \sin\theta}{\sqrt{1 - 4\sin^4\theta/2}}, 0, -\frac{\cos\delta}{\sqrt{1 - 4\sin^4\theta/2}}\right), \tag{6}$$

where ω is a variable describing the rotation between the portions of the side panel above and below DH. Denote by φ the angle between a_5 and a_6. Since $\cos\varphi = a_5 \cdot a_6$,

$$\cos\varphi = \frac{\sin\omega\cos\delta}{\sqrt{1 - 4\sin^4\theta/2}} = \frac{\sin\omega\sqrt{1 - \tan^2\theta/2}}{\sqrt{1 - 4\sin^4\theta/2}} \tag{7}$$

While folding the bag with slit edges, it is always possible to adjust ω so that a_5 and a_6 become the closest, or φ is minimum. It is obvious from equation 7 that the minimum is obtained when $\omega = \pi/2$:

$$\cos\varphi_{\min} = \frac{\sqrt{1 - \tan^2\theta/2}}{\sqrt{1 - \sin^4\theta/2}} \tag{8}$$

Plotting this curve, we find that the maximum gap angle during folding is about 22°. This solution indicates that the box can be folded rigidly provided that additional material can be found to fill the gap; figure 9 shows a conjectured solution.

6.2 Folding Cubical Bags by Twisting

In the special case that $d = h = w$, a "twist" folding scheme can be applied. The crease pattern is shown in figure 10(a) and a card model is displayed in figure 10(b).

The scheme is not applicable to taller bags with a square base – during the fold, corner and midpoints on the top edges of the bag are not co-planar in spite that

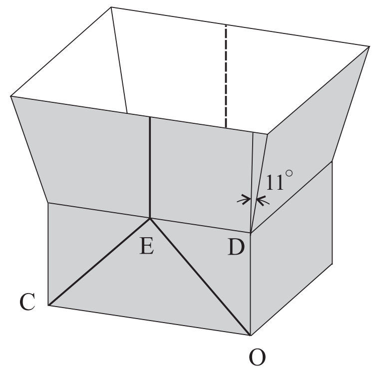

Figure 9: A tall shopping bag with material added to allow folding.

they become co-planar in the fully folded and fully open states. This makes it difficult to join two neighbouring portions of the bag when the same folding scheme applies to both portions. The twist folding scheme is not applicable to bags with a rectangular base do to lack of rotational symmetry.

6.3 Folding by Telescoping

We have considered a few special cases; in this section we show that any tall shopping bag can be collapsed with the addition of a finite number of fixed creases. Theorem 3 will show the procedure. In order to verify the procedure, it is necessary to show that facets do not collide during folding; the primary method for showing this will be to consider the volumes that might be swept by each facet during folding, and to show that these volumes do not intersect.

Theorem 3 *A tall shopping bag can be collapsed with the addition of a finite number of creases.*

Proof: The approach is to shorten the box, by adding creases that allow the top to be rolled inside the box. Once the box is short, theorem 2 allows the box to be collapsed.

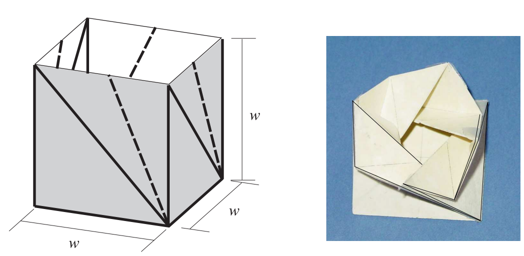

(a) (b)

Figure 10: The 'twist' folding of a cubical bag.

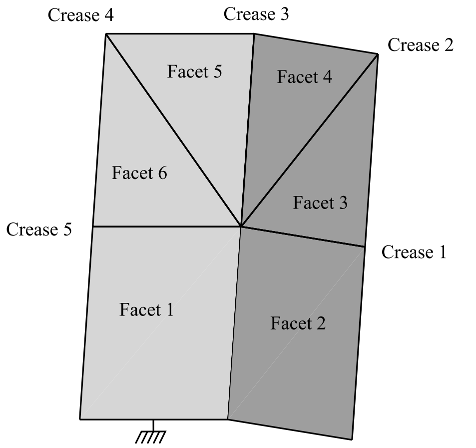

Figure 11: An edge of the shopping bag with creases added to allow folding. Facets 1 and 2 are rigidly connected; there are joints (creases) between all other pairs of adjacent facets.

We consider a single edge of the box, with crease pattern shown in figure 11.

The crease between facets 1 and 2 is fixed at $90°$. The fold takes place in three steps. During step 1, we fix crease 5, and drive crease 3 from $180°$ to $0°$, choosing the solution such that crease angle 1 is positive, crease angle 2 is negative, and crease angle 4 is positive. During step 2, we fix crease 3 at $0°$, and drive crease 1 to $180°$. Crease angles 2 and 4 do not change sign, and crease angle 5 becomes positive. During step 3, we fix crease 1 at $180°$, and drive crease 3 to -180. Crease angles 2 and 4 return to $0°$, and crease angle 5 reaches $180°$. Table 1 summarizes the crease angles after each step.

Ignoring self-intersection, the existence of a trajectory of this form can be verified using the graphical method for determining the topology of of a degree-four spherical linkage, since each of the steps is a fixes two of the six creases (the crease between facets 1 and 2, and one other.)

To prove that self-intersection does not occur, consider pairwise intersections of facets. No two adjacent facets can collide unless the angle of the crease between them crosses $180°$; this never happens for our choice of trajectory. Table 2 summarizes the analysis of collision possibilities for non-adjacent facets.

A single edge can be rolled inside the box using the procedure above; to shorten the box, place symmetric crease patterns at each edge. Figure 12 shows an animation. For a tall box, or a box with dissimilar length and width, it may be necessary to perform a number of shortenings before collapsing the box. Note that the height removed during a shortening can be as small as desired, so it is possible to shorten the box to any desired height. ∎

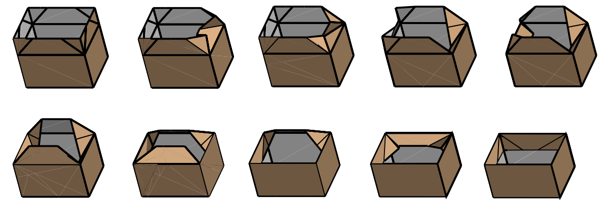

Figure 12: Procedure for shortening a rectangular tube.

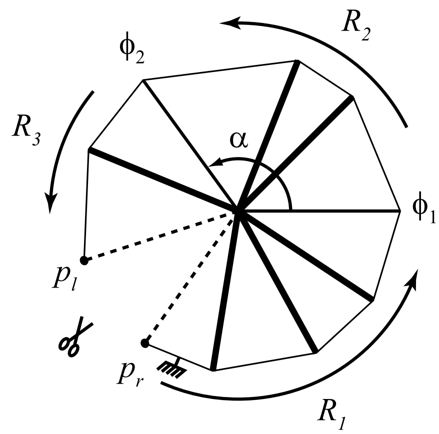

Figure 13: Solving for three dependent crease angles.

7 Relationships Among Crease Angles for Degree-n Vertices

Huffman gives a relationship between opposite dihedral angles for a degree-four vertex, and we have described a graphical method for analyzing the connectedness of the space of configurations for vertices, assuming that self-intersection of the paper is ignored.

In order to permit simulation and analysis of more complicated origami mechanisms, we expect it to be useful to be able to determine the relationship between dihedral angles around vertices of higher degree. This section presents a parameterization of the configurations the paper around a vertex; this parameterization was used to build a simulator for rigid origami, which was used to generate the frames shown in figure 12.

We choose $n-3$ arbitrary independent crease angles as input, and solve for the remaining crease angles. (In the special case where the dependent crease angles are sequential, a simpler solution is possible using the inverse kinematics approach described in [8].)

Figure 13 shows the procedure; φ_1, φ_2, and φ_3 are the crease angles to be solved for. First cut the crease corresponding to φ_3, and flatten the paper. For any valid configuration of the paper, the two cut edges must 'line up' in such a way that they could be re-glued together. Let p_l and p_r be points along these edges a unit distance from

	θ_1	θ_2	θ_3	θ_4	θ_5
Start	$0°$	$0°$	$90°$	$0°$	$0°$
After step 1	$+, < 180°$	$-, > -180°$	$0°$	$+, < 180°$	$0°$
After step 2	$180°$	$-, > -180°$	$0°$	$+, < 180°$	$+, < 180°$
After step 3	$180°$	$0°$	$-180°$	$+, < 180°$	$0°$

Table 1: A trajectory for shortening an edge of a shopping bag.

	facet(s)	vs. facet(s)	Don't intersect because:
Step 1	3	1, 6	Workspace of 3 is a right circular cone that intersects plane of facets 1, 6 only at origin.
	3	5	Workspaces of 3, 5 right circular cones, sep. $\geq 90°$.
	4	1, 2, 6	Facet 4 is bounded by two creases. Crease 2 is inside the box for $\theta_1 \geq 0$, and crease 3 is as well for $\theta_5 = 0, \theta_4 \geq 0$.
	5	2	Workspace of 5 is a right circular cone that intersects plane of facet 2 only at origin.
	5	6	Facet 6 is co-planar with facet 1.
Step 2	4, 5	1, 2	Crease 2 and crease 4 are inside the box for $\theta_1 \geq 0$ and $\theta_5 \geq 0$.
	3	1	Cone workspace vs. plane; intersection is origin.
	3	6	Right circular cone workspaces sep. $\geq 90°$.
	6	2	Cone workspace vs. plane; intersection is origin.
Step 3	6	2, 3	Cone workspace vs. plane.
	6	4	Right circular cone workspaces sep. $\geq 90°$.
	5	1, 2, 3	Creases 3, 4 inside the box for range of θ_2, θ_5.
	4	1	Cone workspace vs. plane.
	4	6	Right circular cone workspaces sep. $\geq 90°$.

Table 2: Summary of collision possiblities for non-adjacent facets while shortening the tall shopping bag.

the vertex.

Anchor the facet clockwise from the φ_3 crease, and choose a coordinate system with origin at the vertex and with the x-axis along the φ_1 crease. The point p_r lies at a fixed position within the $z = 0$ plane in this coordinate system.

If p_l were permitted to move, then its location would be given by a sequence of rotations about each of the creases. Let R_x and R_z be matrices describing rotation about the x and z axes respectively. Let R_1, R_2, and R_3 be matrices corresponding to rotations about the independent crease angles, as shown in figure 13.

The closure constraint can now be written as

$$R_1 R_x(\varphi_1) R_2 R_z(\alpha) R_x(\varphi_2) R_z(-\alpha) R_3 p_l = p_r, \qquad (9)$$

Our goal is to solve for φ_1 and φ_2, given R_1, R_2, and R_3, which may be easily computed from the independent crease angles and the geometry of the paper. Rewrite equation 9:

$$R_x(\varphi_1) Z R_x(\varphi_2) a = b, \qquad (10)$$

where Z, a, and b may be computed:

$$Z = R_2 R_z(\alpha) \qquad (11)$$
$$a = R_z(-\alpha) R_3 p_l \qquad (12)$$
$$b = R_1^T p_r. \qquad (13)$$

Multiplying out equation 10 gives three equations, the first of which is

$$k_3 = k_1 \cos\varphi_2 + k_2 \sin\varphi_2, \qquad (14)$$

with k_1, k_2, and k_3 computed to be

$$k_1 = z_{12} a_2 + z_{13} a_3 \qquad (15)$$
$$k_2 = z_{13} a_2 - z_{12} a_3 \qquad (16)$$
$$k_3 = b_1 - z_{11} a_1. \qquad (17)$$

If $k_1 = k_2 = 0$, then equation 14 implies that φ_2 can take on any value. Otherwise, equation 14 has the solution(s)

$$\varphi_2 = \operatorname{atan}(k_2, k_1) \pm \operatorname{acos}\left(\frac{k_3}{\sqrt{k_1^2 + k_2^2}}\right). \qquad (18)$$

There may be zero, one, two, or infinitely many solutions for φ_2. For each value of φ_2, the remaining two rows of equation 10 can be used to solve for φ_1, which either has a unique value or is unconstrained. φ_3 is uniquely determined by the angle between the normals to the facets at either end of the cut chain.

8 Open problems

We conjecture that it is possible to unfold a paper bag from its flat state if it was already folded using the usual set of creases (by an adversary equipped with techniques from origami or reality).

9 Acknowledgments

Z. You is grateful to the Royal Academy of Engineering from whom he received a Global Research Award that enabled him to work on this most exciting problem.

The idea of gluing two shopping bags together along their tops, as described in the abstract, is due to Robert Lang.

References

[1] D. J. Balkcom and M. T. Mason. Introducing robotic origami folding. In *Proceedings of the 2004 IEEE International Conference on Robotics and Automation*, 2004.

[2] R. Connelly. The rigidity of certain cabled frameworks and the second-order rigidity of arbitrarily triangulated convex surfaces. *Advances in Mathematics*, 37(3):272–299, 1980.

[3] R. Connelly. Rigidity. In *Handbook of Convex Geometry*, volume A, pages 223–271. North-Holland, Amsterdam, 1993.

[4] R. Connelly, I. Sabitov, and A. Walz. The bellows conjecture. *Beiträge zur Algebra und Geometrie (Contributions to Algebra and Geometry)*, 38(1):1–10, 1997.

[5] E. D. Demaine and M. L. Demaine. Computing extreme origami bases. Technical Report CS-97-22, Department of Computer Science, University of Waterloo, Waterloo, Ontario, Canada, May 1997.

[6] E. D. Demaine, S. L. Devadoss, J. S. B. Mitchell, and J. O'Rourke. Continuous foldability of polygonal paper. In *Proceedings of the 16th Canadian Conference on Computational Geometry*, pages 64–67, Montréal, Canada, August 2004.

[7] M. Gardner. Tetraflexagons. In *The Second Scientific American Book of Mathematical Puzzles & Diversions*, chapter 2, pages 24–31. University of Chicago Press, 1987.

[8] L. Han and N. M. Amato. A kinematics-based probabalistic roadmap method for closed chain systems. In *Workshop on the Algorithmic Foundations of Robotics*, pages 233–246, May 2000.

[9] D. Huffman. Curvature and creases: A primer on paper. *IEEE Transactions on Computers*, C-25(10):1010–1019, Oct. 1976.

[10] M. Kapovich and J. Millson. On the moduli space of polygons in the Euclidean plane. *Journal of Differential Geometry*, 42(1):133–164, 1995.

[11] M. E. Knight. Paper bag machine. U.S. Patent 116,842, July 11 1871.

[12] J. M. McCarthy. *Geometric Design of Linkages*, volume 11 of *Interdisciplinary Applied Mathematics (Systems and Control)*. Springer-Verlag, 1995.

[13] R. J. Milgram and J. Trinkle. The geometry of configurations spaces for closed chains in two and three dimensions. *Homology, Homotopy, and Applications*, forthcoming.

[14] sarah-marie belcastro and T. C. Hull. Modelling the folding of paper into three dimensions using affine transformations. *Linear Algebra and its Applications*, 348:273–282, June 2002.

[15] I. Streinu and W. Whiteley. The spherical carpenter's rule problem and conical origami folds. In *Proceedings of the 11th Annual Fall Workshop on Computational Geometry*, Brooklyn, New York, November 2001.

[16] J. Trinkle and R. J. Milgram. Complete path planning for closed kinematic chains with spherical joints. *International Journal of Robotics Research*, 21(9):773 – 789, Dec. 2002.